Supporting Information

Afzal et al. 10.1073/pnas.1423588112

SI Materials and Methods

Flow Cytometry. Single cell suspensions were prepared from thymus, spleen, or LN. Spleen and LN suspensions were treated with red blood cell (RBC) lysis buffer to remove erythrocytes. Cells ($1–2 \times 10^6$) were preincubated with Fc block for 15 min at 4 °C and stained with antibodies (Abs) recognizing: CD16/CD32 (2.4G2), CD25 (PC61), CD45R/B220 (RA3-6B2), CD69 (H1.2F3), CD4, CD8a, CD44, CD62L, TCRβ, CD5, CD3, NK1.1, CD11c, CD11b, GR-1, CD45.1, CD45.2, PD-1, CD127, or CD95 (all from BD Biosciences or eBioscience unless otherwise specified). Flow cytometry data were acquired using either a FACSCalibur (BD) or FACSCanto (BD) flow cytometer, and analyzed with either CellQuest software (BD) or FlowJo 7.5 software (Tree Star).

Intracellular Flow Cytometry. Permeabilization and intracellular staining to detect Foxp3, IL-17A, or IFNγ were performed using the appropriate Cytofix/Cytoperm kits (BD Biosciences) according to the manufacturer's instructions. Flow cytometry was performed as above.

DNA Damage-Induced Apoptosis. Cells were exposed to apoptotic stimuli as detailed in the main text and cultured overnight in RPMI complete medium. Apoptosis was evaluated by Annexin V/7-AAD or Annexin/PI staining using standard protocols.

^{3}H-Thymidine Incorporation. Purified naïve T cells were seeded into U-bottom 96-well plates that were precoated with the concentrations of anti-CD3 and anti-CD28 Abs indicated in the figures. ^{3}H-thymidine (1 μCi) was added to each well and cells were cultured for another 8 h, after which proliferation was determined at 72 h by measuring ^{3}H-thymidine uptake using a liquid scintillation β-counter (TopCount reader).

Transmission Electron Microscopy (TEM). Naïve T cells were cultured overnight in medium alone, or in plates precoated with 10μg/mL anti-CD3 Ab plus 1 μg/mL anti-CD28 Ab plus chloroquine (25 μM). Cells were fixed in 1.5% glutaraldehyde/1.5% (vol/vol) paraformaldehyde using standard procedures. Fixed cells were processed for TEM and examined using a Philips TEM instrument by the EM facility at the Hospital for Sick Children, Toronto.

CFSE Dilution. Purified T cells were washed twice with PBS without calcium or magnesium ($PBS^{-/-}$) and incubated with 1 μM CFSE for 15 min at 37 °C. The labeling reaction was stopped with cold FBS, and excess CFSE was removed by two additional washes in $PBS^{-/-}$. For evaluation of reconstitution in lymphopenic hosts, $UR^{fl/fl}$ ($CD45.1^+$) and $UR^{fl/fl}$;*Lck-Cre* ($CD45.2^+$) cells were mixed 1:1 and labeled with CSFE as described above. Labeled mixed cells (5×10^6) were i.v. injected into lethally irradiated (10 Gy) CD45.1/2 C57BL/6 recipient mice and CFSE dilution was assessed as above.

Lymphopenia-Induced Homeostatic Proliferation. Purified, naive T cells from $UR^{fl/fl}$ ($CD45.1^+$) and $UR^{fl/fl}$;*Lck-Cre* ($CD45.2^+$) mice were labeled with CFSE as described above. Labeled cells were mixed 1:1 and 5×10^6 cells were i.v. injected into lethally irradiated CD45.1/2 C57BL/6 recipient mice.

In vitro $CD4^+$ Th Effector Cell Differentiation. In vitro differentiation of Th effector cell subsets was induced as described (1).

EAE Induction. EAE was induced in mice and disease severity scored as described (1).

LCMV Infections. Mice (8-12 wk old) were i.v.-injected with 10^5 pfu Armstrong LCMV strain. PBL samples were obtained over the course of the infection and numbers of $CD8^+$ T cells, GP33 tetramer-specific $CD8^+$ T cells, NP396 tretramer-specific $CD8^+$ T cells, and $CD4^+$ T cells were determined by flow cytometric analysis of the appropriate markers and tetramers. The MHC I: GP33-41 H2-Db and NP396–404H2-Db tetramers were kindly provided by Dr. Pamela Ohashi (University Health Network). Some mice were killed on day 8 postinfection and splenocytes were subjected to parallel immunophenotyping, GP33 restimulation, and tetramer analyses.

Viral Titres. Viral titres were determined using a plaque-forming assay as described (2).

Statistics. Where appropriate, all differences were evaluated using the unpaired 2-tailed Student's t test, as calculated using GraphPad Prism software. Data are presented as mean ± SEM unless otherwise indicated. Differences of at least $P < 0.05$ were considered statistically significant.

1. Brüstle A, et al. (2012) The NF-κB regulator MALT1 determines the encephalitogenic potential of Th17 cells. *J Clin Invest* 122(12):4698–4709.

2. Battegay M, et al. (1991) Quantification of lymphocytic choriomeningitis virus with an immunological focus assay in 24- or 96-well plates. *J Virol Methods* 33(1-2):191–198.

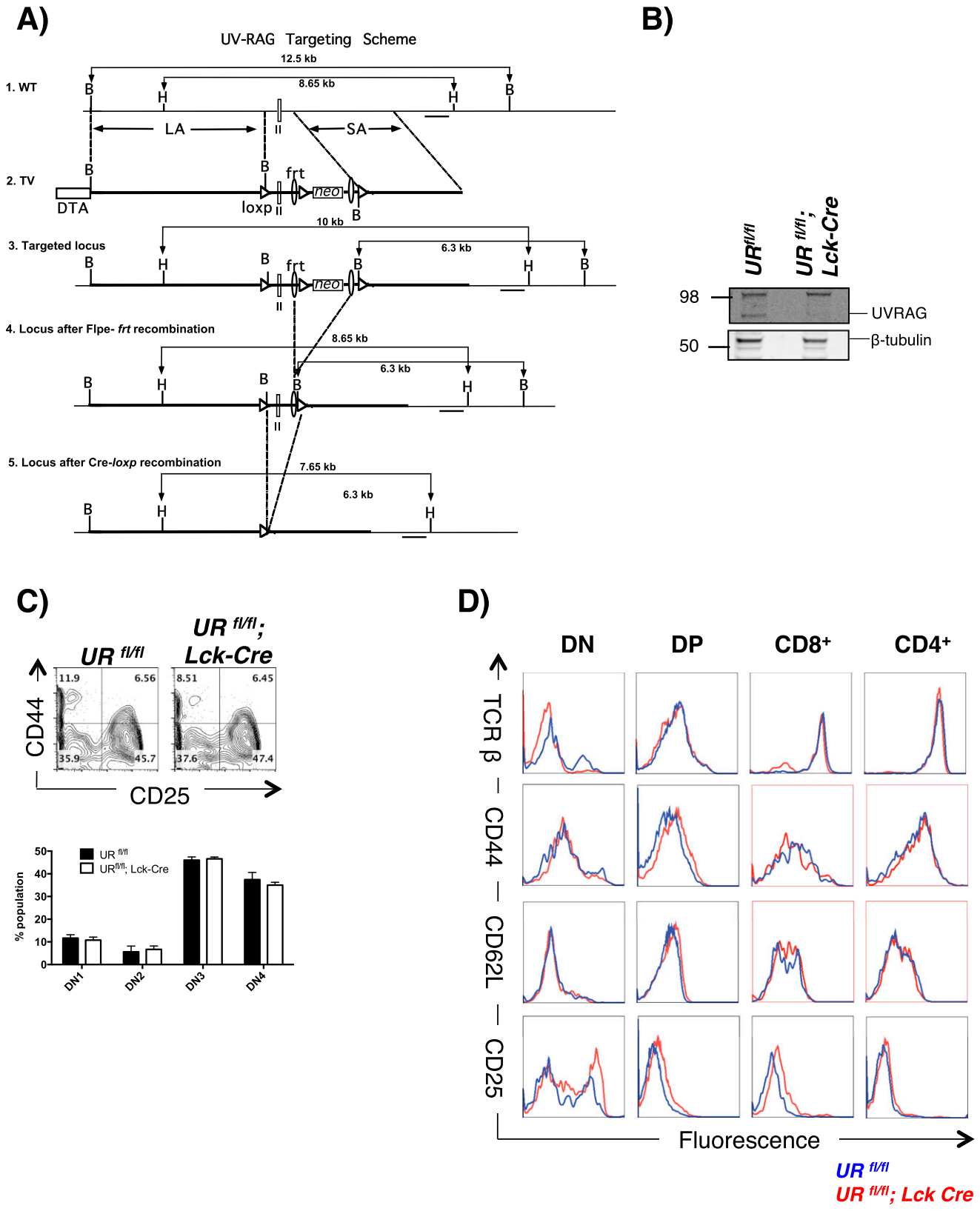

Fig. S1. Generation and validation of conditional *Uvrag*-deficient mice, and thymocyte analysis. (*A*) Schematic diagram of conditional targeting of the mouse *Uvrag* gene. 1, WT murine genomic *Uvrag* locus. The long arm (LA) and short arm (SA) of homology are indicated, as is *Uvrag* exon II, which is essential for UVRAG function. Probes used to verify targeting events are marked by short horizontal lines, and the expected sizes of restriction fragments are shown. H, HindIII; B, BamHI. 2, Targeting vector (TV) design. LoxP sites (triangles) were inserted to flank *Uvrag* exon II and the neomycin resistance gene (*neo*), which was used as a selection marker. DTA, Diphtheria toxin A. 3, Targeted *Uvrag* allele. 4, Locus after Flpe-frt-mediated removal of *neo*. 5. Locus after Cre

Legend continued on following page

recombinase-mediated removal of *Uvrag* exon II. (*B*) Immunoblot confirming loss of UVRAG protein in peripheral T cells purified from $UR^{fl/fl}$;*Lck-Cre* mice. $UR^{fl/fl}$, littermate control. β-tubulin, loading control. Results are representative of at least three trials involving 2–4 mice per genotype. (*C*) (*Upper*) Flow cytometric analysis of DN thymocyte stages in thymus of littermate $UR^{fl/fl}$ and $UR^{fl/fl}$;*Lck-Cre* mice. Numbers in quadrants are percentages of lineage negative ($CD4^-CD8^-CD3^-$) cells that were DN1 ($CD44^+CD25^-$), DN2 ($CD44^+CD25^+$), DN3 ($CD44^-CD25^+$), or DN4 ($CD44^-CD25^-$) cells. Results are representative of three mice per group. (*Lower*) Quantitation of mean percentages ± SEM of the indicated DN thymocyte subsets from three $UR^{fl/fl}$ and 3 $UR^{fl/fl}$; *Lck-Cre* mice. (*D*) Flow cytometric profiling of the indicated markers in the indicated thymocyte subsets isolated from thymi of $UR^{fl/fl}$ (blue line; control) and $UR^{fl/fl}$;*Lck-Cre* (red line) mice. Results are representative of at least three independent experiments involving 1–4 mice per group.

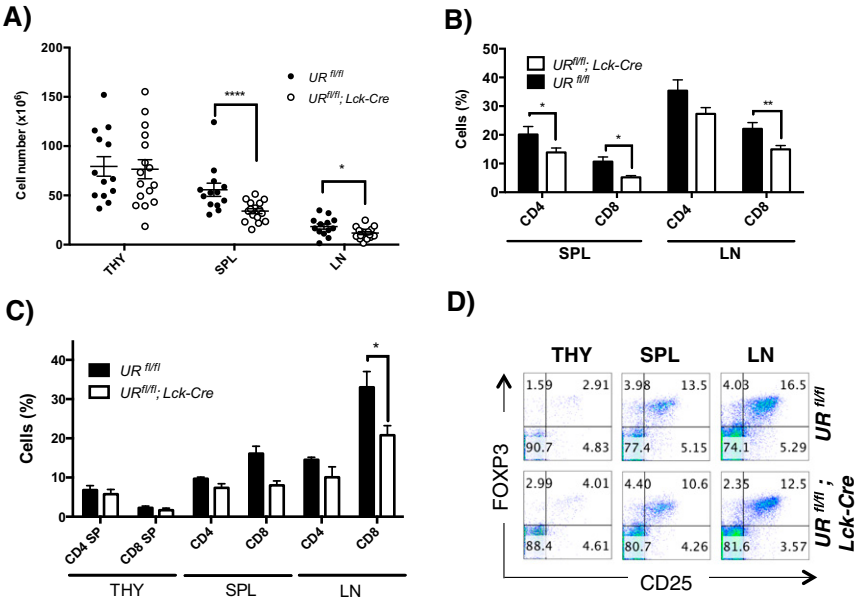

Fig. S2. Loss of UVRAG does not impair T-cell maturation. (*A*) Quantitation of absolute cellularity of the thymus (THY), spleen (SPL), and lymph nodes (LN) of $UR^{fl/fl}$ and $UR^{fl/fl}$;*Lck-Cre* mice. Each data point represents an individual mouse. Horizontal lines are the cumulative geometric mean ± SEM of 13 independent experiments involving 1–4 mice per group. (*B*) Quantitation of percentages of $CD4^+$ and $CD8^+$ T cells in SPL and LN of $UR^{fl/fl}$ and $UR^{fl/fl}$;*Lck-Cre* mice. Data are the cumulative mean ± SEM of 13 independent experiments involving 1–4 mice per group. (*C*) Quantitation of percentages of the indicated cell subsets in THY, SPL and LN of aged $UR^{fl/fl}$ and $UR^{fl/fl}$;*Lck-Cre* mice (>6 mo old, $n = 3$ mice per group). Results are the mean ± SEM $*P < 0.05$. (*D*) Flow cytometric analysis of $CD25^+FoxP3^+$ regulatory T cells (Tregs) in THY, SPL, and LN of $UR^{fl/fl}$ and $UR^{fl/fl}$;*Lck-Cre* mice ($n = 1$–2 per group). Numbers are percentages of total $CD4^+$ T cells. Results are representative of three independent experiments.

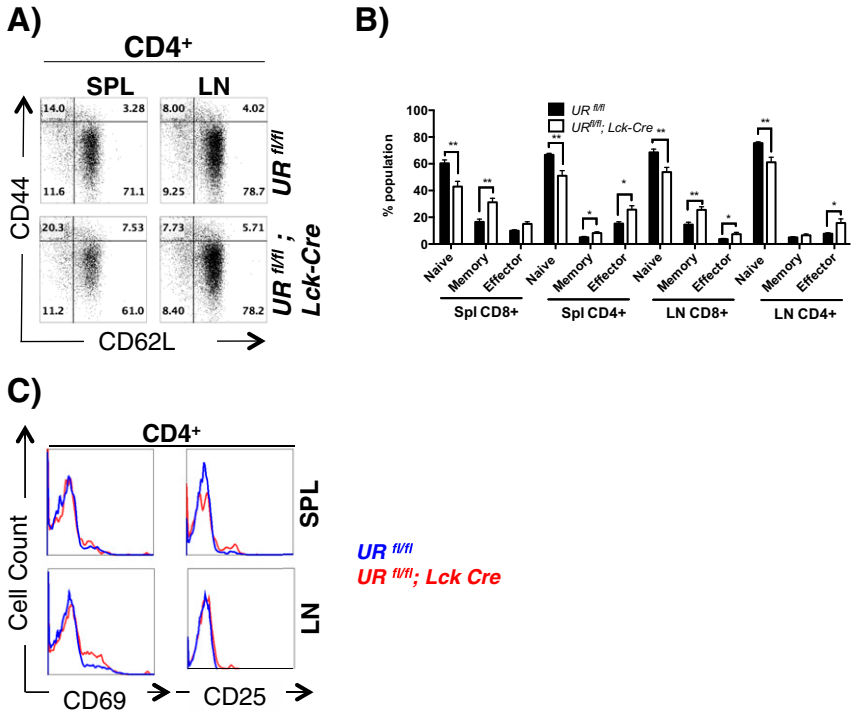

Fig. S3. Altered marker profile of residual UVRAG-deficient T cells. (*A*) Flow cytometric analysis of T cells from SPL and LN of littermate $UR^{fl/fl}$ and $UR^{fl/fl}$;*Lck-Cre* mice ($n = 1$–4 per group) that were immunophenotyped to detect the activation/memory markers CD44 and CD62L. Numbers are percentages of total $CD4^+$ T cells and are representative of eight trials. (*B*) Quantitation of flow cytometric data for the mice in *A* and Fig. 3*A*, distinguishing among naïve ($CD62L^+CD44^-$), memory ($CD62L^+CD44^+$), and effector ($CD62L^-CD44^+$) T cells in SPL and LN. Results are the mean ± SEM and are representative of eight independent experiments involving 1–4 mice/genotype. $^*P < 0.05$; $^{**}P < 0.005$. (*C*) Flow cytometric plots of CD69 and CD25 expression by T cells from SPL and LN of littermate $UR^{fl/fl}$ and $UR^{fl/fl}$;*Lck-Cre* mice. Data are representative of six independent experiments involving 1–4 mice per genotype.

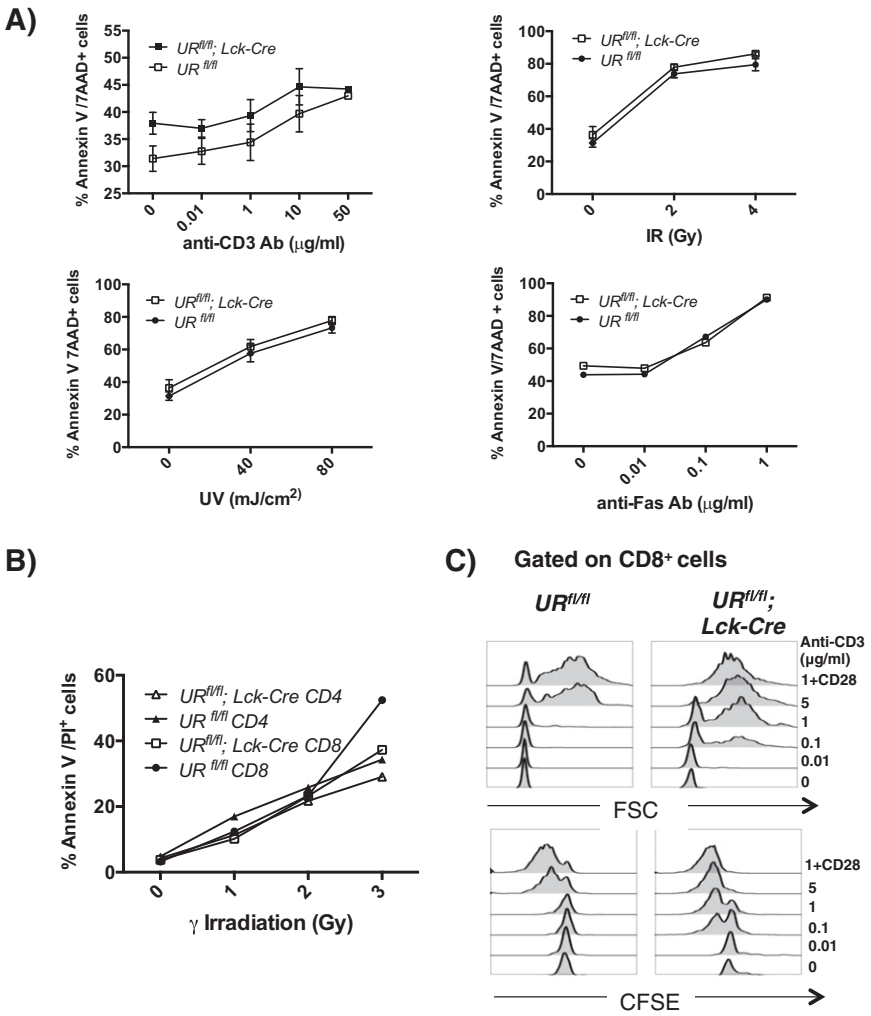

Fig. S4. Normal T-cell apoptosis but hyperproliferation of *UR*$^{fl/fl}$*;Lck-Cre* T lineage cells. (*A*) Quantitation of apoptosis in thymocytes that were isolated from *UR*$^{fl/fl}$ or *UR*$^{fl/fl}$*;Lck-Cre* mice ($n = 3$ per group) and treated with indicated levels of plate-bound anti-CD3 antibody (Ab), UV radiation, γ-irradiation (IR; Gy), or anti-Fas Ab. Cells were cultured overnight after treatment and apoptosis was measured by Annexin V/7AAD staining and flow cytometry. Data are the mean ± SEM ($n = 3$) and are representative of two trials. (*B*) Quantitation of apoptosis in cultures of CD4$^+$ or CD8$^+$ T cells that were isolated from SPL of *UR*$^{fl/fl}$ or *UR*$^{fl/fl}$*;Lck-Cre* mice ($n = 1$ per group), treated with indicated amounts of IR, and cultured overnight. Apoptosis was measured as in *A*. Data were obtained from a single experiment. (*C*) Flow cytometric analysis of the proliferation of naïve CD8$^+$ T cells that were labeled in vitro with CFSE (1 μM) and treated with the indicated concentrations of plate-bound anti-CD3/CD28 Abs for 72 h. Both FSC (*Upper*) and CFSE (*Lower*) profiles are shown. Results are representative of at least three independent trials involving 2–4 mice per group.

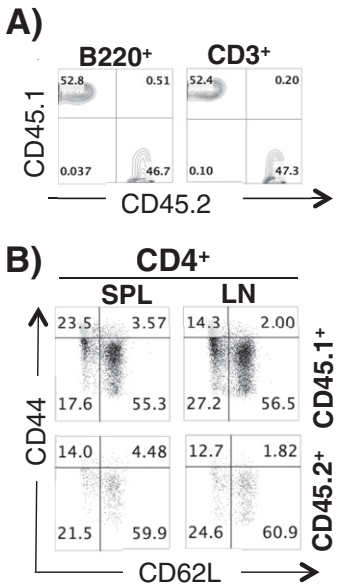

Fig. S5. UVRAG-deficient T cells show a defect in bone marrow reconstitution. (*A*) Flow cytometric analysis of B220$^+$ and CD3$^+$ cell populations in PBL of *UR*$^{fl/fl}$:*UR*$^{fl/fl}$ BM chimeras. After 1.5–2 mo, BM reconstitution was assessed by measuring the relative contribution of *UR*$^{fl/fl}$ (CD45.1$^+$) and *UR*$^{fl/fl}$ (CD45.2$^+$) BM cells to the regeneration of B (B220$^+$) and T (CD3$^+$) cell populations in PBL. Numbers are percentages of live B220$^+$ or CD3$^+$ cells. Results are representative of three trials. (*B*) Flow cytometric analysis of CD44 and CD62L expression by T cells from SPL and LN of mixed BM chimeras containing *UR*$^{fl/fl}$ (CD45.1$^+$) and *UR*$^{fl/fl}$;*Lck-Cre* (CD45.2$^+$) donor BM cells (n = 3 mice). Data were analyzed as in Fig. 3*D*. Numbers are percentages of total CD4$^+$ T cells and are representative of two trials.

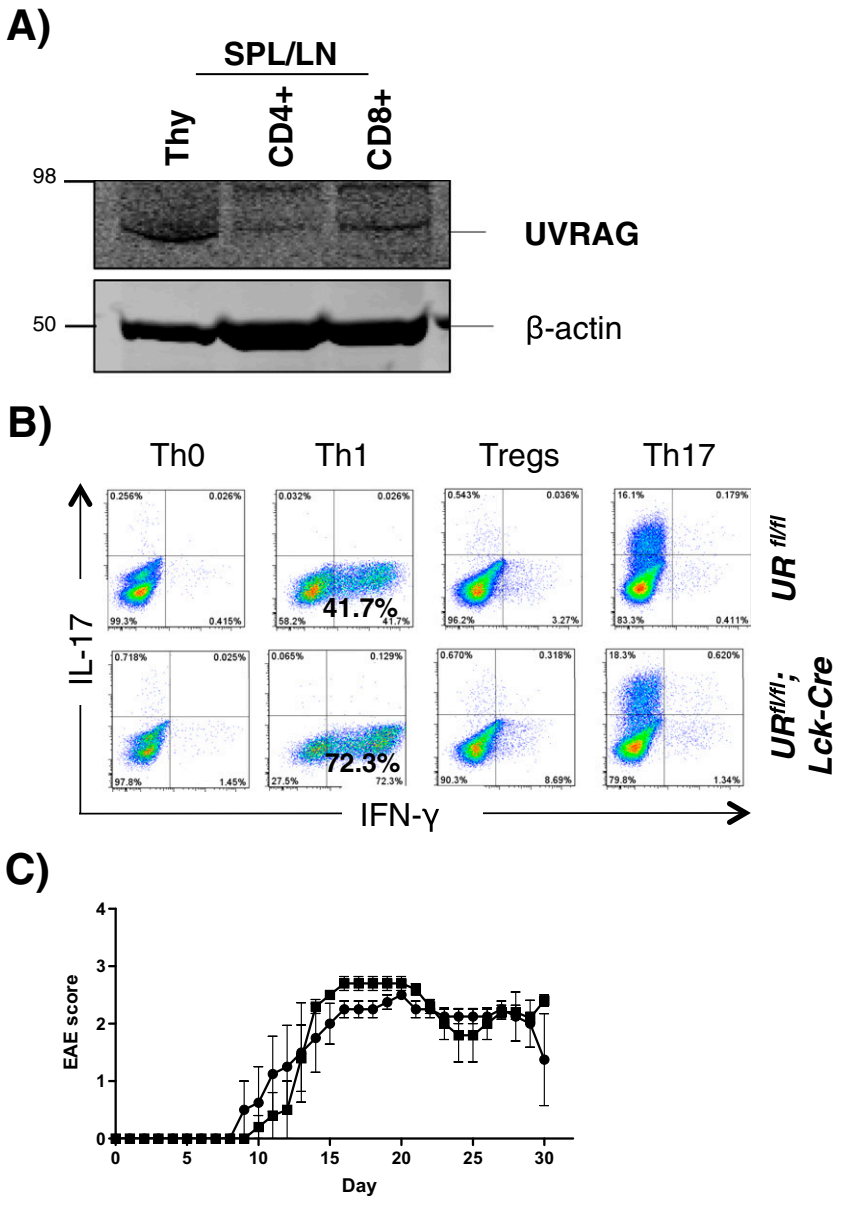

Fig. S6. UVRAG deficiency does not prevent mice from developing EAE. (*A*) Immunoblot to detect UVRAG protein in lysates of thymocytes (Thy) and purified $CD4^+$ and $CD8^+$ T peripheral cells pooled from SPL and LN of a $UR^{fl/fl}$ mouse. Top band, nonspecific protein. β-actin, loading control. Results are representative of two independent experiments each involving 2–3 $UR^{fl/fl}$ mice. (*B*) Flow cytometric analysis of in vitro Th effector cell differentiation by naïve $CD4^+$ T cells that were purified from $UR^{fl/fl}$ or $UR^{fl/fl}$;*Lck-Cre* mice ($n = 1$ per group) and cultured in mixtures of Th subset-specific cytokines (1) in the presence of anti-CD3/CD28 Abs plus IL-2. Th cells were restimulated in vitro with PMA/ionomycin for 6 h, followed by intracellular staining to detect IFNγ (Th1 cells), Foxp3 (Tregs), and IL-17 (Th17 cells). Th0 cells were identified by their lack of cytokine secretion. Numbers are percentages of live $CD4^+$ T cells. Results are representative of two independent experiments. (*C*) Analysis of EAE scores of $UR^{fl/fl}$ (circles) and $UR^{fl/fl}$;*Lck-Cre* (squares) mice ($n = 5$ per group) that were immunized s.c. with MOG peptide in complete Freund's adjuvant, followed by i.p. injection of pertussis toxin. Mice were scored daily for EAE disease severity (1). Data are the cumulative mean ± SEM of two independent experiments each involving five mice per genotype.

1. Brüstle A, et al. (2012) The NF-κB regulator MALT1 determines the encephalitogenic potential of Th17 cells. *J Clin Invest* 122(12):4698–4709.

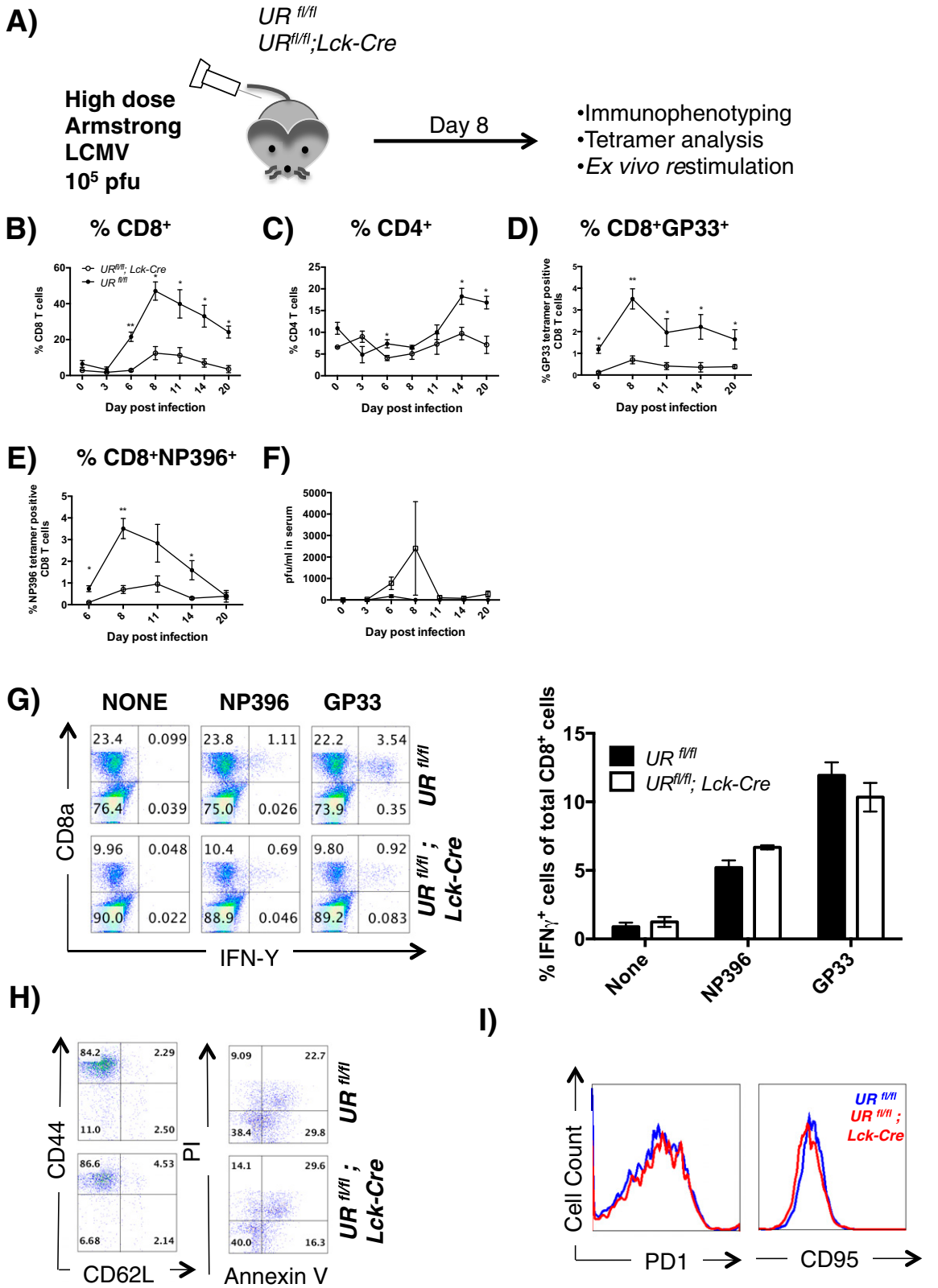

Fig. S7. Altered T-cell response to LCMV infection in $UR^{fl/fl}$;*Lck-Cre* mice. (*A*) Schematic diagram of acute LCMV infection protocol. $UR^{fl/fl}$ and $UR^{fl/fl}$;*Lck-Cre* mice (6–8 wk old; $n = 3$ per group) were injected with LCMV (10^5pfu) and the indicated analyses were performed on day 8 postinfection. (*B–E*) PBL samples from the mice in *A* were drawn on the indicated days postinfection and the percentages of cells in these samples that were total $CD8^+$ T cells (*B*), total $CD4^+$ T cells (*C*), GP33 tetramer-specific $CD8^+$ T cells (*D*), and NP396 tetramer-specific $CD8^+$ T cells (*E*) were determined by flow cytometry. Results are mean ± SEM (n = 2–3 per group) and are representative of one trial. (*F*) Quantitation of viral titres in serum of the mice in *A*. Results are the mean ± SEM (n = 2–3 per group). (*G*) (*Left*) Flow cytometric analysis of the percentage of IFNγ-producing $CD8^+$ T cells among splenocytes that were isolated from LCMV-infected $UR^{fl/fl}$ or

Legend continued on following page

UR$^{fl/fl}$*;Lck-Cre* mice (n = 3 per group) and stimulated in vitro for 5 h with no peptide (None), or with NP396 or GP33 peptide. IFNγ production was detected by intracellular staining. Plots are gated on live CD8$^+$ T cells and numbers in upper right quadrants represent IFNγ-producing CD8$^+$ T cells. Data were obtained from one trial. (*Right*) Quantitation of IFNγ-producing CD8$^+$ T cells among the splenocytes in the left panel. Results are the mean ± SEM (n = 3 per group) and were obtained from one trial. (*H*) (*Left*) Flow cytometric analysis of CD44 and CD62L expression by the CD8$^+$ splenocytes in Fig. 5*A*. (*Right*) Flow cytometric analysis of apoptotic cells among the CD8$^+$ splenocytes in Fig. 5*A*. (*I*) Flow cytometric plot of PD-1 (*Left*) and Fas (*Right*) expression by the CD8$^+$ splenocytes in Fig. 5*A*.